TELKOMNIKA Telecommunication Computing Electronics and Control
Vol. 24, No. 6, December 2026, pp. 1884~ 1894
ISSN: 1693-6930, DOI: 10.12928/TELKOMNIKA.v24i6.28074

Local-area differential global positioning system performance in equatorial Indonesia using elevation-based weighting model

Septian Ridho Syah Putra[1], Jelia Anita[1], Tri Budi Santoso[1], Meiditomo Sutyarjoko[2], Djaka Ariya Putra Ketti[2]
[1]Department of Electrical Engineering, Politeknik Elektronika Negeri Surabaya, Surabaya, Indonesia
[2]PT. Pasifik Satelit Nusantara, Bekasi, Indonesia

Article Info

Article history:

Received May 25, 2026
Revised Sep 16, 2026
Accepted Oct 11, 2026

Keywords:

Differential global positioning system
Equatorial Indonesia
Global navigation satellite system
Local-area differential global positioning system
Multipath mitigation
Weighted least squares

ABSTRACT

This study evaluates the effectiveness of elevation-based weighted least squares (WLS) for local-area differential global positioning system (LADGPS) against conventional least squares (LS) and signal-to-noise ratio (SNR)-based WLS on a heterogeneous public Indonesian continuously operating reference station (Ina-CORS) network in equatorial Indonesia. Using 24-hour pseudorange observations from the Indonesian geospatial reference system (SRGI) across baselines ranging from 7 to 143 km, the proposed approach was assessed under varying local multipath conditions. At a rover station affected by severe local multipath, conventional LS produced a 3D root mean square error (RMSE) of 1.24 m, which was reduced to 0.92 m using elevation-based WLS, while SNR-based WLS achieved 0.75 m. Across the complete network, however, elevation-based WLS outperformed SNR-based WLS at six of nine rover stations, with comparable mean RMSE reductions of 0.166 m and 0.179 m, demonstrating more consistent performance on heterogeneous receiver infrastructure through its hardware-independent geometric weighting. These results indicate that the evaluated elevation-based WLS model provides a robust and practical weighting strategy for LADGPS in heterogeneous equatorial CORS networks, achieving sub-meter positioning accuracy even at baselines exceeding 140 km.

This is an open access article under the CC BY-SA license.

Corresponding Author:

Septian Ridho Syah Putra
Department of Electrical Engineering, Politeknik Elektronika Negeri Surabaya
Raya ITS St., Keputih, Sukolilo, Surabaya, East Java
Email: septianridho@pasca.student.pens.ac.id

1. INTRODUCTION

Single-frequency positioning in the global navigation satellite system (GNSS) remains widely used for its simple architecture [1], but its accuracy is highly susceptible to atmospheric delay. In equatorial regions such as Indonesia, the equatorial ionization anomaly (EIA) causes elevated positioning errors [2], [3]. Built-in atmospheric models such as Klobuchar and Saastamoinen are commonly applied in standard point positioning (SPP) [4]–[6]; however, the Klobuchar model reduces only about 50% of ionospheric error near the equator [7], [8] leaving residual errors at the meter level.

Local-area differential global positioning system (LADGPS) mitigates this by exploiting spatially correlated atmospheric errors between reference and rover stations [9]. However, its effectiveness is constrained by spatial decorrelation, with a practical limit conventionally cited at approximately 100 km [10]. Empirical evaluation of this limit under the complex ionospheric conditions of equatorial continuously operating reference station (CORS) networks, particularly in Indonesia, remains rare. After differential

correction, spatially uncorrelated errors, receiver noise and local multipath, remain dominant despite suppression of common-mode errors such as orbital and clock bias [11]. As these residuals become the primary contributor to positioning uncertainty, the quality of individual satellite observations plays an increasingly critical role in position estimation.

Most prior differential global positioning system (DGPS) studies rely on conventional least squares (LS) processing, which assigns uniform weight to all satellite observations regardless of quality [12], [13]. This assumption is particularly inappropriate for low-elevation satellites, which are more susceptible to atmospheric residuals, multipath, and signal attenuation [14]. Adaptive weighting schemes have been proposed to address this, most commonly based on signal-to-noise ratio (SNR) [15], while more recent approaches have explored carrier-phase-informed stochastic models [16] and machine learning-based weighting derived from observation residual patterns [17]. However, these methods typically require dual-frequency observations or extensive training datasets, both of which fall outside the scope of the single-frequency processing framework adopted in this study. Although SNR-based weighting can track signal degradation directly, its effectiveness depends heavily on receiver hardware characteristics; a reliability comparison against geometric elevation-based weighting has not yet been examined at the scale of a heterogeneous public CORS network under equatorial conditions.

This study addresses this gap through a comprehensive empirical evaluation of existing weighting strategies, namely standard LS, SNR-based weighted least squares (WLS), and elevation-based WLS for single-frequency LADGPS processing in equatorial Indonesia. Unlike prior evaluations conducted on homogeneous receiver networks or under mid-latitude conditions [13], [18], and without accounting for instrument heterogeneity in weighting reliability [19], this study specifically investigates how receiver heterogeneity influences the reliability of stochastic weighting models on the heterogeneous Indonesian CORS (Ina-CORS) network of the Indonesian geospatial reference system (SRGI), using real pseudorange data across baselines up to 140 km. A deliberately degraded 0° elevation mask serves as a stress test to expose each algorithm's robustness limits under low-elevation and multipath-affected observations. The primary contribution is empirical evidence that SNR-based weighting's effectiveness is contingent on receiver-reported signal-quality consistency, whereas the deterministic, hardware-agnostic elevation-based model sustains more consistent stability while maintaining sub-meter positioning accuracy.

2. METHOD

2.1. DGPS standard model

DGPS relies on differential corrections computed at a reference station with precisely known coordinates to correct rover observations [10]. The reference station computes the difference between its observed pseudorange and the true geometric range to each satellite, defined as the pseudorange correction (PRC), which is mathematically expressed as (1):

$$PRC^s(t) = P_b^s(t) - \rho_b^s(t) \quad (1)$$

where $P_b^s(t)$ is the reference-station pseudorange and $\rho_b^s(t)$ is the true geometric range to satellite s. This correction, capturing common-mode errors such as satellite clock, orbital, and atmospheric delay biases at the reference location, is subtracted from the corresponding rover pseudorange, equivalent in effect to inter-receiver single-differencing; the remaining residual is dominated by the relative receiver clock error, residual ionospheric and tropospheric decorrelation, and observation noise and local multipath. Rover position is then estimated via LS as (2):

$$\Delta x = (H^T H)^{-1} H^T \Delta\rho \quad (2)$$

where H is the satellite geometry matrix, and Δx the position and receiver clock correction vector [10]. Conventional LS assigns uniform weight to all observations, making the solution vulnerable to high-noise, low-elevation satellites affected by local multipath, the limitation addressed by the weighted approach in subsection 2.2.

2.2. Observation weighting models

Incorporating a weighting matrix W into the position estimation, the (3) generalizes the LS solution to a weighted form, where W is an $n \times n$ diagonal matrix whose elements w_i represent the weight assigned to the i-th satellite observation, with off-diagonal terms equal to zero [10]. Each diagonal element is calculated as the inverse of the observation's estimated error variance as (4):

$$\Delta x = (H^T W H)^{-1} H^T W \Delta\rho \tag{3}$$

$$w_i = \frac{1}{\sigma_i^2} \tag{4}$$

2.3. Elevation-based weighting model

In GNSS observations, the satellite elevation angle is closely related to the quality of the observation signal. Satellites at low elevations are generally more susceptible to multipath effects, signal attenuation, and residual atmospheric errors. To account for these characteristics, this study applies an elevation-based observation variance model following the approach in [20]:

$$\sigma_i^2 = a^2 + \left(\frac{b}{\sin E_i}\right)^2 \tag{5}$$

where E_i is the elevation angle of the i-th satellite, while a and b represent the constant error component and the error component dependent on the satellite's elevation, respectively. The parameter $a = 0.3$ m represents the standard deviation of the L1 coarse/acquisition code (C/A) pseudorange noise under ideal conditions, which is consistent with the pseudorange accuracy characteristics of standard GPS receivers [10]. The parameter $b = 0.5$ m was chosen to represent the elevation-dependent error component in single-frequency pseudorange observations [21]. These parameter values were adopted based on established literature on GNSS stochastic modeling rather than empirically tuned for this dataset.

Based on (4), (5) satellites at low elevation (close to 0°) will mathematically produce a large error variance σ_i^2, causing the resulting final weight, w_i to approach zero. This mechanism automatically reduces the influence of high-noise observations from low-elevation satellites without discarding data via a high elevation mask. To evaluate the robustness of the fixed elevation-based parameters, a sensitivity analysis was conducted by varying each parameter individually ($a \in \{0.2, 0.3, 0.4\}\, m$; $b \in \{0.3, 0.5, 0.7\}\, m$) while holding the other at its baseline value and evaluating the resulting network-average and station-specific 3D root mean square error (RMSE). Results are presented in subsection 3.2.

2.4. SNR-based weighting model

For performance comparison, this study also implements a model that directly links signal strength parameters to the variance of the observation error. The mathematical formulation for the SNR model is given by (6):

$$\sigma_i^2 = a + b \cdot 10^{-0.1 \cdot SNR_i} \tag{6}$$

Following the validated approach, the empirical parameter values used are $a = 1$ and $b = 10^5$. As these values were adopted directly from the validated formulation of [15] without modification, they were not subjected to a separate sensitivity analysis in this study. This exponential relationship ensures that any decrease in SNR due to environmental interference significantly increases $\sigma_i{}^2$, with the corresponding weight computed via (4), so that signals experiencing local distortion are adaptively suppressed during position estimation.

2.5. System architecture and processing pipeline

To evaluate the proposed algorithm, a LADGPS post-processing framework was developed using the Python programming language. The system architecture shown in Figure 1 consists of three main subsystems: differential correction generation, rover observation processing, and position estimation. The corresponding processing procedure, including epoch synchronization, satellite validity checks, and the iterative estimation loop, is formalized in Algorithm 1. The iterative WLS procedure invoked in Algorithm 1 (line 6) is detailed in Algorithm 2, which incorporates the elevation- and SNR-based weighting models defined in (5), (6). Each iteration in Algorithm 2 involves inversion of an $n \times n$ weight matrix, where n corresponds to the number of tracked satellites (typically fewer than 15); this operation is computationally trivial ($O(n^3)$ per epoch) and executes in well under 1 ms on standard hardware, making total processing time dominated by I/O rather than parameter estimation.

Although the current framework operates in post-processing mode using static receiver independent exchange format (RINEX) files, this computational cost imposes no fundamental barrier to real-time operation. Extending the framework to real-time applicability would primarily require replacing static file parsing with a live networked transport of RTCM via internet protocol (NTRIP) / radio technical commission for maritime services (RTCM) streaming interface, while the core PRC generation and WLS estimation logic (Algorithm 1 and Algorithm 2) remain unchanged.

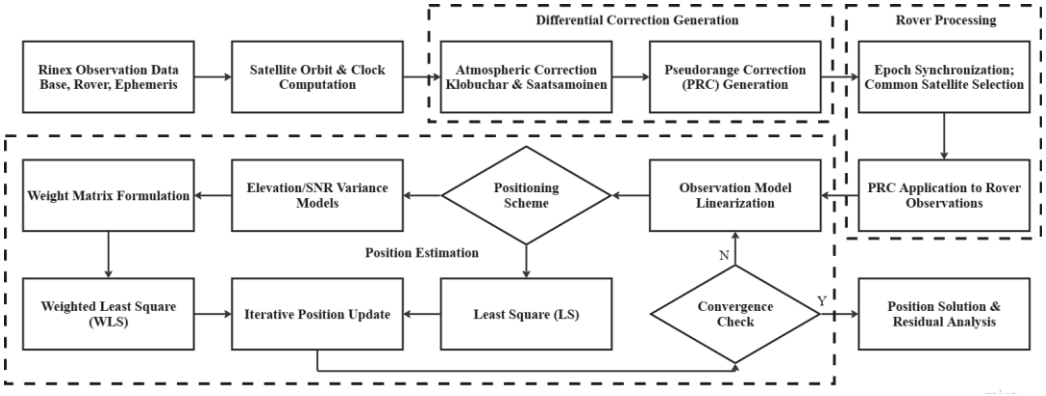


Figure 1. System architecture and processing pipeline of the proposed LADGPS framework

```
Algorithm 1: DGPS-WLS main pipeline
Input: Reference/rover observations, broadcast ephemeris NAV, reference position X_ref,
       initial rover position X0, weighting mode (Elevation/SNR)
Output: Estimated rover position X_rov(t)
1: Parse reference/rover OBS & NAV
2: Match epochs by timestamp tolerance
3: for each matched epoch t do
4:       S ← common satellites with valid PRC (|S|≥4); else skip epoch
5:       X ← previous solution or X0
6:       X ← Solve iterative WLS position estimation
             (Algorithm 2)
7:       Apply post-fit rejection (if enabled)
8:       Store X, residuals, weights, QC status
9: end for
```

```
Algorithm 2: Iterative WLS position estimation
Input: Corrected rover pseudorange, satellite positions X_sat^s, initial position X0,
       weighting mode (Elevation/SNR)
Output: X, residuals, W, Q
1: X ← X0; clock ← 0
2: repeat
3:     for each satellite s: compute R^s, Δρ^s, H_s, elevation E_s, weight w_s
4:     W ← diag(w_s)
5:     Δx ← (H^T WH)^-1 H^T WΔρ
6:     X ← X + Δx_xyz; clock ← clock + Δx_clock
7: until ‖Δx_xyz‖ < ε=1×10^-4 or max_iteration reached
8: Q ← (H^T WH)^-1
9: return X, residuals, W, Q
```

2.6. Observation data and research design

This study utilizes 24-hour RINEX observations collected on 15 January 2026 from the SRGI CORS network. A radial baseline configuration was adopted, with the Surabaya station (CSBY) as the reference and nine surrounding stations as rovers, spanning baseline distances of 7-143 km. This configuration enables systematic evaluation of spatial decorrelation effects while isolating baseline distance and local environmental conditions as the primary sources of performance variation, as CSBY provides stable, continuous data availability. Reference coordinates for each rover were obtained from official SRGI publications and used as ground truth for accuracy evaluation. Configuration and processing parameters are summarized in Table 1.

Table 1. Experiment configuration parameters and data processing

Parameter	Configuration
Observation time	January 15, 2026
Duration of observation	24 hours
Constellation	GPS
Signal	Single-frequency (L1 C/A)
Ephemeris	Broadcast ephemeris
Ionospheric model	Klobuchar
Tropospheric model	Saastamoinen
Elevation mask	0°

Processing incorporated broadcast ephemerides with uniformly applied atmospheric corrections: the Klobuchar model for ionospheric delay [7] and the Saastamoinen model for tropospheric delay [22]. A key design choice was setting the elevation mask to 0°. Unlike standard geodetic processing, which typically excludes satellites below 10°-15° to avoid severe low-horizon multipath [23]–[25], this zero-degree masking was intentionally applied to test WLS robustness against signal degradation from local multipath and low-elevation observations, conditions representative of obstructed environments such as urban canyons, forested terrain, or mountainous regions, where usable satellites are inherently constrained to low elevation angles regardless of receiver hardware class.

To verify that the observation day was representative of typical equatorial ionospheric conditions, the rate of total electron content index (ROTI) was computed from L1/L2 RINEX observations at all nine rover stations for January 15, 2026. Median ROTI values ranged from 0.048 to 0.096 TECU/min, with 95th-percentile values below 0.24 TECU/min, and only 1.1–3.4% of epochs exceeding the 0.5 TECU/min threshold conventionally associated with ionospheric irregularity onset [26]. These results indicate quiet-to-stable local ionospheric conditions, supporting the observation day as representative rather than anomalous. Figure 2 shows the spatial distribution of the reference station and nine rover stations, all located within East Java Province, Indonesia.



Figure 2. Spatial distribution of the reference station and 9 rover stations within the Ina-CORS network

Beyond their spatial distribution, the nine rover stations also differ substantially in underlying receiver and antenna hardware. Table 2 summarizes the receiver, antenna, and radome configuration of each station, extracted from its RINEX header, confirming instrumental heterogeneity in contrast to the receiver-homogeneous configurations typically assumed in prior mid-latitude studies [13], [18].

Table 2. Receiver and antenna configuration of the Ina-CORS stations used in this study

Station	Receiver	Antenna
CSID	Leica GR50	LEIAR20
CMJT	Trimble Alloy	TRM159900.00
CPAS	Leica GR50	LEIAR20
CMLG	Leica GR50	LEIAR20
CBGO	Trimble Alloy	TRM159900.00
CNGA	Trimble Alloy	TPSCR.G3
CPMS	Trimble Alloy	TRM159900.00
CLUM	Leica GR50	LEIAR20
CMAG	Trimble Alloy	TRM159900.00

3. RESULTS AND DISCUSSION

3.1. LADGPS performance and the effects of spatial decorrelation

The first evaluation compares SPP with LADGPS using the conventional LS algorithm, examining how differential corrections from the CSBY reference station reduce common errors and how spatial decorrelation limits accuracy as baseline distance increases. Overall, LADGPS provided a marked accuracy improvement over SPP. Under SPP with LS, 3D RMSE ranged from 4.1-4.8 m, dominated by equatorial ionospheric bias that the Klobuchar model could not fully remove. After DGPS correction, 3D errors were reduced by an average of 80%, confirming the effectiveness of differential correction in eliminating spatially correlated atmospheric biases and enabling sub-meter accuracy at most stations.

Testing at extreme distances, however, revealed departures from the common assumption that DGPS accuracy degrades linearly with baseline distance due to spatial decorrelation [27], [28]. As shown in Table 3, CMAG, despite the longest baseline (143 km), maintained a 3D RMSE of 0.84 m. Its clear-sky environment, largely free of local signal reflections, suggests that the remaining residual error is primarily attributable to atmospheric spatial decorrelation rather than local multipath.

Table 3. Comparison of RMSE from SPP and DGPS using LS algorithm

Reference station	Rover	Baseline (km)	SPP (m)			DGPS (m)			3D error reduction (%)
			H	V	3D	H	V	3D	
CSBY	CSID	7	2.13	4.11	4.63	0.51	0.8	0.94	79.5%
	CMJT	34	1.97	3.87	4.34	0.4	0.73	0.83	80.7%
	CPAS	40	1.93	3.75	4.22	0.35	0.67	0.76	81.9%
	CMLG	71	2.05	4.35	4.81	0.6	1.08	1.24	74.2%
	CBGO	88	2.06	4.2	4.68	0.42	0.94	1.03	77.8%
	CNGA	95	1.89	3.68	4.14	0.41	0.73	0.84	79.6%
	CPMS	102	1.99	4.2	4.64	0.4	0.74	0.84	81.8%
	CLUM	106	1.9	3.73	4.18	0.37	0.71	0.8	80.7%
	CMAG	143	1.91	3.67	4.14	0.41	0.74	0.84	79.6%

Conversely, the most severe degradation occurred at CMLG, a moderate-distance station (71 km) well within the conventional 100 km DGPS limit, yet producing the worst 3D RMSE (1.24 m). This indicates that local multipath and signal attenuation near the rover antenna, intentionally exposed via the 0° elevation mask, can outweigh baseline-distance effects. The standard LS algorithm's uniform weighting of all satellites, including noisy low-elevation ones, underscores the need for an adaptive weighting scheme to isolate such local anomalies.

This contrast is further evident in the post-fit pseudorange residual distributions shown in Figure 3. At CMAG, residual percentile bands remained tight even at low elevation, with σ below 15° of 0.403 m. In contrast, CMLG exhibited a marked widening of residuals, with σ below 15° increasing to 0.938 m alongside frequent clipped outliers. To quantify this local multipath contribution, a code-minus-carrier multipath and receiver-noise indicator (MP1/MP2) was computed from L1/L2 RINEX observations at all nine rover stations. Among all stations, CMLG exhibited the highest standard deviation of leveled MP1 at low elevation angles (<15°), reaching 0.281 m, approximately 1.55 times higher than at CMAG (0.181 m) and twice its own high-elevation value (0.140 m, ≥15°). A consistent pattern was observed for MP2, where CMLG reached 0.566 m compared with 0.303 m at CMAG (1.87 times higher). These results confirm that the residual widening at CMLG is associated with genuinely elevated low-elevation code multipath and receiver noise rather than an artifact of the positioning algorithm, although comparable degradation was also observed at a subset of other stations (e.g., CSID), suggesting local multipath variability is a broader characteristic of the heterogeneous network. This attribution is further supported by the quiet ionospheric conditions established for the observation day (subsection 2.4), reducing the likelihood that ionospheric decorrelation contributed to the anomaly and reinforcing local multipath as the dominant error source at CMLG.

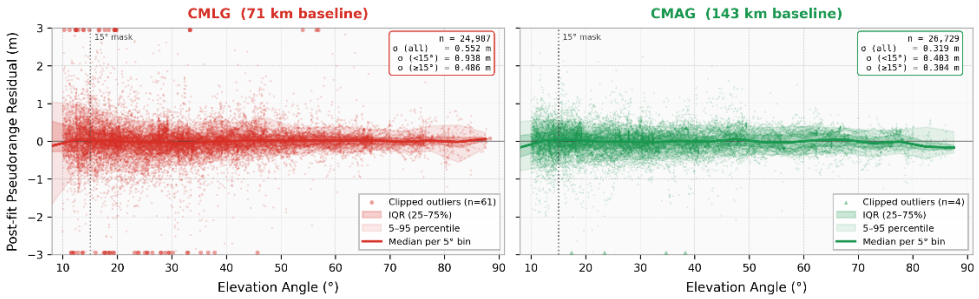


Figure 3. Post-fit pseudorange residual distributions at CMLG and CMAG using DGPS LS

3.2. Performance evaluation and comparative analysis of weighting models

The adaptive weighting mechanism effectively addressed the sensitivity of conventional LS to signal-quality variation. Table 4 shows that WLS consistently improved LADGPS positioning accuracy at all

nine rover stations, with the largest gains in the vertical component, reflecting its effectiveness against satellite-geometry limitations at low elevation.

Table 4. Comparison of RMSE from DGPS using LS, WLS-SNR and WLS-elevation algorithm

Reference station	Rover	Baseline (km)	LS (m)			WLS-SNR (m)			WLS-elevation (m)		
			H	V	3D	H	V	3D	H	V	3D
CSBY	CSID	7	0.51	0.8	0.94	0.35	0.56	0.66	0.38	0.61	0.72
	CMJT	34	0.4	0.73	0.83	0.35	0.63	0.72	0.35	0.62	0.71
	CPAS	40	0.35	0.67	0.76	0.28	0.53	0.6	0.27	0.52	0.59
	CMLG	71	0.6	1.08	1.24	0.34	0.67	0.75	0.44	0.81	0.92
	CBGO	88	0.42	0.94	1.03	0.37	0.8	0.88	0.35	0.77	0.85
	CNGA	95	0.41	0.73	0.84	0.35	0.66	0.74	0.34	0.63	0.72
	CPMS	102	0.4	0.74	0.84	0.38	0.62	0.73	0.37	0.63	0.73
	CLUM	106	0.37	0.71	0.8	0.3	0.6	0.67	0.28	0.58	0.65
	CMAG	143	0.41	0.74	0.84	0.36	0.67	0.76	0.35	0.66	0.74

At CMLG, the station most affected by local multipath, LS produced the highest 3D RMSE of 1.24 m. WLS-elevation reduced the error to 0.92 m, demonstrating the benefit of accounting for satellite elevation in the weighting process. Meanwhile, WLS-SNR achieved the largest reduction, reaching 0.75 m, indicating that SNR-based weighting more directly captures severe signal-quality degradation than a purely geometric approach.

To evaluate the robustness of the fixed elevation-based parameters ($a = 0.3$ m, $b = 0.5$ m) underlying this result, a sensitivity analysis was conducted, varying each parameter individually while holding the other at baseline in Table 5. Both the network-average and CMLG-station RMSE varied only marginally, ranging from 0.737 to 0.746 m and from 0.924 to 0.961 m, respectively, confirming that the reported results are not narrowly dependent on the specific parameter values adopted. Decreasing b to 0.3 m produced the largest degradation, indicating that under-weighting the elevation-dependent term reduces the model's ability to suppress low-elevation noise. For practitioners lacking site-specific calibration data, values of a within 0.2-0.3 m and b within 0.5-0.7 m provide comparable, robust stability without requiring precise tuning.

Table 5. Sensitivity of WLS-elevation parameters on positioning accuracy

Station	*a* (m)	*b* (m)	Avg. 3D RMSE (m)	CMLG 3D RMSE (m)
Baseline	0.3	0.5	0.737	0.924
Low a	0.2	0.5	0.739	0.931
High a	0.4	0.5	0.743	0.948
Low b	0.3	0.3	0.746	0.961
High b	0.3	0.7	0.739	0.932

At the network scale, however, WLS-elevation proved more consistently stable, achieving the best accuracy at six of the nine rover stations (CMJT, CPAS, CBGO, CNGA, CLUM, and CMAG). This pattern suggests that WLS-SNR performance is hardware-dependent, sensitive to variation in receivers, antennas, and C/N0 reporting across public CORS networks, whereas the universal geometric basis of elevation weighting makes it more robust to such instrumental heterogeneity.

A Wilcoxon signed-rank test on the station-level 3D RMSE of nine stations, summarized in Table 6, confirmed that both WLS methods significantly outperformed LS, with p = 0.0039 for both comparisons, the smallest two-sided value attainable for this sample size. Across all nine stations, WLS-SNR and WLS-elevation reduced RMSE by an average of 0.179 m and 0.166 m, respectively. No statistically significant difference was found between WLS-SNR and WLS-elevation (p = 0.711), corroborating the absence of a universally superior model observed above.

Figure 4 corroborates these findings at the distributional level: both WLS methods narrow the residual spread and reduce outliers relative to LS, with WLS-SNR showing the tightest distribution at the anomalous CMLG station and WLS-elevation showing greater consistency across the full network. From an operational standpoint, the RMSE reductions summarized in Tables 3 and 4, and illustrated in Figures 3 and 4, carry direct practical significance: station-level accuracy shifts from the 0.76–1.24 m range under conventional LS to a consistently sub-meter range (0.59–0.92 m) under WLS, moving results from a marginal, near-1-meter classification to a reliably sub-meter tier relevant for applications such as cadastral boundary verification and lane-level navigation, where the 1 m threshold often determines practical usability.

Table 6. Wilcoxon signed-rank test comparing station-level 3D RMSE ($n = 9$)

Comparison	Mean diff. (m)	W	p-value	Outcome
LS vs WLS-SNR	0.179	0.000	0.0039	Significant (SNR wins 9/9)
LS vs WLS-elevation	0.166	0.000	0.0039	Significant (elevation wins 9/9)
WLS-SNR vs WLS-elevation	−0.013	15.000	0.711	Not significant (elevation 6/9, SNR 2/9)

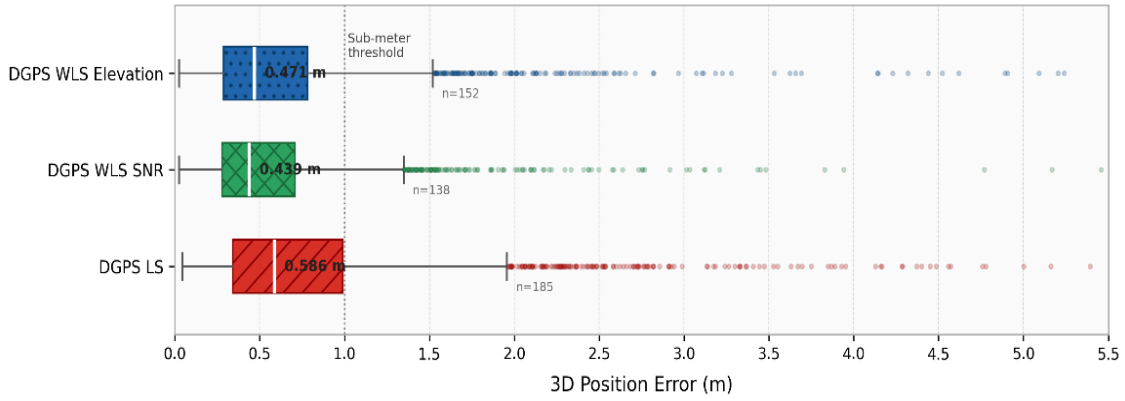


Figure 4. 3D positioning error distribution at CMLG under DGPS-LS, WLS-SNR, and WLS-elevation

Taken together, the results of this study indicate that neither model is universally superior, and that the optimal choice of weighting scheme is context-dependent. WLS-SNR is more appropriate when severe, localized multipath degradation is present and receiver hardware is known to report reliable C/N0 values. WLS-elevation, by contrast, offers a more robust and hardware-agnostic alternative for deployment across heterogeneous public CORS networks, where receiver-dependent variability in SNR reporting may undermine the reliability of signal quality indicators. This distinction constitutes a practical design guideline for LADGPS implementations in equatorial regions where both infrastructure heterogeneity and multipath variability are prevalent, though based on a single quiet-ionosphere day and not validated under disturbed conditions.

4. CONCLUSION

This study shows that receiver hardware heterogeneity, rather than baseline distance, governs weighting-model reliability in public CORS networks, a gap unaddressed by prior LADGPS research on homogeneous, mid-latitude deployments. Across nine heterogeneous Ina-CORS stations under a deliberately degraded 0° elevation mask, conventional LS accuracy degradation proved driven more by local multipath than spatial decorrelation, evidenced by a 3D RMSE anomaly of 1.24 m at the moderate-baseline (71 km) CMLG station. The two weighting models showed complementary, statistically validated strengths: SNR-based weighting achieved the largest reduction at CMLG (0.75 m) by responding directly to severe local degradation, while elevation-based weighting was more consistently stable network-wide, outperforming SNR at six of nine stations, and robust to parameter variation.

These findings support national geospatial applications such as cadastral surveying and infrastructure mapping across Indonesia's expanding Ina-CORS infrastructure. Future work should extend this evaluation to multi-constellation processing to test whether hardware-independence persists across broader signal environments, hybrid elevation–SNR schemes that adapt to detected anomaly severity, and real-time validation incorporating dual-frequency observations across multiple days and seasons.

ACKNOWLEDGMENTS

The authors would like to thank the Indonesian Geospatial Information Agency (BIG) for providing GNSS observation data. In addition, the authors extend their sincere gratitude to PT. Pasifik Satelit Nusantara (PSN) for their guidance, technical support, and in-depth discussions throughout the research process. Furthermore, the authors gratefully acknowledge PT. Konsultan Satelit Indonesia (KSI) for providing financial support for the publication of this research.

FUNDING INFORMATION

This work was supported by PT. Pasifik Satelit Nusantara and PT. Konsultan Satelit Indonesia.

AUTHOR CONTRIBUTIONS STATEMENT

This journal uses the Contributor Roles Taxonomy (CRediT) to recognize individual author contributions, reduce authorship disputes, and facilitate collaboration.

Name of Author	C	M	So	Va	Fo	I	R	D	O	E	Vi	Su	P	Fu
Septian Ridho Syah Putra	✓	✓	✓	✓	✓	✓		✓	✓	✓	✓		✓	
Jelia Anita	✓	✓		✓	✓			✓		✓	✓		✓	
Tri Budi Santoso	✓	✓		✓				✓		✓		✓	✓	
Meiditomo Sutyarjoko	✓			✓		✓		✓		✓		✓		
Djaka Ariya Putra Ketti	✓	✓		✓	✓	✓		✓		✓		✓		

C : **C**onceptualization
M : **M**ethodology
So : **So**ftware
Va : **Va**lidation
Fo : **Fo**rmal analysis
I : **I**nvestigation
R : **R**esources
D : **D**ata Curation
O : Writing - **O**riginal Draft
E : Writing - Review & **E**diting
Vi : **Vi**sualization
Su : **Su**pervision
P : **P**roject administration
Fu : **Fu**nding acquisition

CONFLICT OF INTEREST STATEMENT

The authors declare that they have no conflict of interest.

DATA AVAILABILITY

The raw data supporting this study are available from the SRGI at https://srgi.big.go.id/. Derived data are available from the corresponding author upon reasonable request.

REFERENCES

[1] A. Grenier, E. S. Lohan, A. Ometov, and J. Nurmi, "A survey on low-power GNSS," *IEEE Communications Surveys and Tutorials*, vol. 25, no. 3, pp. 1482–1509, Dec. 2024, doi: 10.1109/COMST.2023.3265841.

[2] Y. Otsuka, P. Abadi, K. Hozumi, and A. Almahi, "Equinoctial asymmetry of plasma bubble occurrence and electric field at evening: GPS and ionosonde measurements in Southeast Asia," *International Journal of Geoinformatics*, vol. 252, p. 106136, Dec. 2024, doi: 10.1016/j.jastp.2023.106136.

[3] M. C. O. Caldeira, C. R. T. Caldeira, S. S. D. A. Cereja, D. B. M. Alves, and C. R. de Aguiar, "Evaluation of the gnss positioning performance under influence of the ionospheric scintillation," *International Journal of Geoinformatics*, vol. 26, no. 3, pp. 1–19, Dec. 2024, doi: 10.1590/s1982-21702020000300014.

[4] F. Wu, L. Wei, H. Luo, F. Zhao, X. Ma, and B. Ning, "T-SPP: improving GNSS single-point positioning performance using transformer-based correction," *International Journal of Geoinformatics*, vol. 2024, pp. 1–15, Dec. 2024, doi: 10.1155/2024/6643723.

[5] A. Angrisano, S. Ascione, G. Cappello, C. Gioia, and S. Gaglione, "Application of 'Galileo high accuracy service' on single-point positioning," *International Journal of Geoinformatics*, vol. 23, no. 9, p. 4223, Dec. 2024, doi: 10.3390/s23094223.

[6] L. Benvenuto, T. Cosso, and G. Delzanno, "An adaptive algorithm for multipath mitigation in GNSS positioning with android smartphones," *Sensors*, vol. 22, no. 15, p. 5790, Aug. 2022, doi: 10.3390/s22155790.

[7] J. A. Klobuchar, "Ionospheric time-delay algorithm for single-frequency GPS users," *International Journal of Geoinformatics*, vol. AES-23, no. 3, pp. 325–331, Dec. 2024, doi: 10.1109/TAES.1987.310829.

[8] Y. V. Yasyukevich *et al.*, "Klobuchar, NeQuickG, BDGIM, GLONASS, IRI-2016, IRI-2012, IRI-Plas, NeQuick2, and GEMTEC Ionospheric models: a comparison in total electron content and positioning domains," *International Journal of Geoinformatics*, vol. 23, no. 10, p. 4773, Dec. 2024, doi: 10.3390/s23104773.

[9] K. Krasuski, D. Popielarczyk, A. Ciećko, and J. Ćwiklak, "A new strategy for improving the accuracy of aircraft positioning using dgps technique in aerial navigation," *International Journal of Geoinformatics*, vol. 14, no. 15, p. 4431, Dec. 2024, doi: 10.3390/en14154431.

[10] P. K. Enge, "The global positioningsystem: signals, measurements, and performance," *International Journal of Geoinformatics*, vol. 1, no. 2, pp. 83–105, Dec. 2024, doi: 10.1007/BF02106512.

[11] T. L. Dammalage, "Effects of site-dependent errors on the accuracy of C/A code DGPS positioning," *International Journal of Geoinformatics*, vol. 4, no. 10, pp. 2296–2304, Dec. 2024, doi: 10.28991/cej-03091159.

[12] T. Phasinam *et al.*, "Real-time monitoring and positioning of agricultural tractors using a low-cost GPS and IoT device," *International Journal of Geoinformatics*, vol. 21, no. 1, pp. 111–120, Dec. 2024, doi: 10.52939/ijg.v21i1.3799.

[13] M. Bakuła, M. Uradziński, and K. Krasuski, "Performance of DGPS smartphone positioning with the use of P(L1) vs. P(L5) pseudorange measurements," *International Journal of Geoinformatics*, vol. 14, no. 4, p. 929, Dec. 2024, doi: 10.3390/rs14040929.

[14] N. I. Muhammad, M. Y. Abdullahi, and Y. S. Abu, "A review of the effects of low elevation angles on the propagation for satellite communication link," *Fudma Journal of Sciences*, vol. 7, no. 1, pp. 170–175, Dec. 2024, doi: 10.33003/fjs-2023-0701-1270.
[15] J. Li and M. Wu, "The improvement of positioning accuracy with weighted least square based on SNR," *Proceedings - 5th International Conference on Wireless Communications, Networking and Mobile Computing, WiCOM 2009*, pp. 1–4, Dec. 2024, doi: 10.1109/WICOM.2009.5302600.
[16] P. Liu, K. V. Ling, H. Qin, X. Jiang, and J. Lu, "Optimal selection of elevation-dependent stochastic models for real-time PPP with GPS/Galileo/BDS," *International Journal of Geoinformatics*, vol. 73, no. 9, pp. 4571–4583, Dec. 2024, doi: 10.1016/j.asr.2024.01.036.
[17] L. Li, M. Elhajj, Y. Feng, and W. Y. Ochieng, "Machine learning based GNSS signal classification and weighting scheme design in the built environment: a comparative experiment," *International Journal of Geoinformatics*, vol. 4, no. 1, Dec. 2024, doi: 10.1186/s43020-023-00101-w.
[18] M. Aquino *et al*., "Improving the GNSS positioning stochastic model in the presence of ionospheric scintillation," *International Journal of Geoinformatics*, vol. 83, no. 10, pp. 953–966, Dec. 2024, doi: 10.1007/s00190-009-0313-6.
[19] K. Parvazi, S. Farzaneh, and A. Safari, "The mathematical weighting of GNSS observations based on different types of receivers/antennas and environmental conditions," *International Journal of Geoinformatics*, vol. 14, no. 5, pp. 521–540, Dec. 2024, doi: 10.1016/j.geog.2023.04.001.
[20] W. Dai, Q. Qi, W. Yu, C. Cai, B. Zheng, and J. Pan, "A robust stochastic model for GNSS real-time kinematic positioning in challenging environments via combining elevation-angle, C/N0, and PLD," *International Journal of Geoinformatics*, vol. 76, no. 11, pp. 6847–6862, Dec. 2024, doi: 10.1016/j.asr.2025.09.039.
[21] C. C. J. M. Tiberius and F. Kenselaar, "Estimation of the stochastic model for GPS code and phase observables," *International Journal of Geoinformatics*, vol. 35, no. 277, pp. 441–454, Dec. 2024, doi: 10.1179/sre.2000.35.277.441.
[22] J. Saastamoinen, "Atmospheric correction for the troposphere and stratosphere in radio ranging of satellites," *International Journal of Geoinformatics*, pp. 247–251, Dec. 2024, doi: 10.1029/GM015p0247.
[23] Z. Zhang, Y. Li, X. He, W. Chen, and B. Li, "A composite stochastic model considering the terrain topography for real-time GNSS monitoring in canyon environments," *International Journal of Geoinformatics*, vol. 96, no. 10, Dec. 2024, doi: 10.1007/s00190-022-01660-7.
[24] H. Ren, G. Li, J. Geng, F. Wang, and P. Li, "Multipath hemispherical map model with geographic cut-off elevation constraints for real-time GNSS monitoring in complex environments," *International Journal of Geoinformatics*, vol. 27, no. 4, Dec. 2024, doi: 10.1007/s10291-023-01530-5.
[25] H. Xu, X. Chen, J. Ou, and Y. Yuan, "Crowdsourcing RTK: a new GNSS positioning framework for building spatial high-resolution atmospheric maps based on massive vehicle GNSS data," *International Journal of Geoinformatics*, vol. 5, no. 1, Dec. 2024, doi: 10.1186/s43020-024-00135-8.
[26] I. Cherniak, I. Zakharenkova, and A. Krankowski, "IGS ROTI Maps: current status and its extension towards equatorial region and southern hemisphere," *International Journal of Geoinformatics*, vol. 22, no. 10, p. 3748, Dec. 2024, doi: 10.3390/s22103748.
[27] D. Weng, S. Ji, Y. Lu, W. Chen, and Z. Li, "Improving DGNSS performance through the use of network rtk corrections," *International Journal of Geoinformatics*, vol. 13, no. 9, p. 1621, Dec. 2024, doi: 10.3390/rs13091621.
[28] M. F. Mohd Yazair, T. A. Musa, W. A. Wan Aris, I. A. Musliman, and A. H. Omar, "Network DGPS accuracy assessment at west coast peninsular Malaysia," *International Journal of Geoinformatics*, vol. 6, no. 24, pp. 301–311, Dec. 2024, doi: 10.35631/jistm.624028.

BIOGRAPHIES OF AUTHORS



Septian Ridho Syah Putra is a student in the Applied Master's Program in Electrical Engineering at Politeknik Elektronika Negeri Surabaya, Indonesia. He earned his Bachelor of Applied in Telecommunications Engineering from Politeknik Elektronika Negeri Surabaya in 2025. His research interests focus on telecommunications signal processing including GNSS positioning and radio frequency, information and communication technology security and software development. He is currently a researcher working on applied research in GNSS signal processing for accurate positioning. He can be contacted at email: septianridho@pasca.student.pens.ac.id.



Jelia Anita is a student in the Applied Master's Program in Electrical Engineering at Politeknik Elektronika Negeri Surabaya, Indonesia. She earned her Bachelor of Applied in Electrical Engineering from Politeknik Elektronika Negeri Surabaya in 2025. Her research interests focus on software engineering, including mobile apps development, artificial intelligence, and internet of things. She is currently a researcher working on applied research in GNSS signal processing for accurate positioning. She can be contacted at email: jeliaanita1007@pasca.student.pens.ac.id.



Tri Budi Santoso was born in Tulungagung, East Java, Indonesia, in 1970. He received his B.Eng. degree in Engineering Physics, his M.T. degree in Electrical Engineering, and his Doctoral degree from the Institut Teknologi Sepuluh Nopember, Surabaya, Indonesia, in 1994, 1999, and 2016, respectively, with research focused on signal processing. He has been with the Department of Electrical Engineering at the Electronic Engineering Polytechnic Institute of Surabaya (PENS) from 1995 until 2021. Since 2021, he has been working with the Creative Multimedia Technology Department at the same University. His research interests include telecommunications and acoustic signal processing. He can be contacted at email: tribudi@pens.ac.id.



Meiditomo Sutyarjoko received his B.Eng. degree in Telecommunications Engineering from Institut Teknologi Bandung (ITB), Indonesia, in 1988. He then earned his M.Sc. degree in Information Science from the USC Viterbi School of Engineering, USA, in 1994, and his Doctoral degree (Ph.D.) in Strategic Management from Universitas Indonesia (UI), Indonesia, in 2010. He has managed more than 20 satellite projects. He began his career in 1989 at Hughes Space and Communication Inc. (USA) and later served as Deputy Vice President of the Space Division at IPTN. He has held various senior executive roles, including President Director of PT Sarana Mukti Adijaya and Lead Consultant for the BRIsat satellite project. In 2022, he was nominated by the Indonesian government for the ITU Radio Regulations Board (RRB). His research interests include ICT technology and business management, strategic management in ICT, and satellite technology and regulation. He can be contacted at email: meiditomo.sutyarjoko@ifg.id.



Djaka Ariya Putra Ketti received the Bachelor degree in Aerospace Engineering from Institut Teknologi Bandung, in 2017. He is currently an Assistant Manager of Spacecraft Engineer at Department of Satellite Bus and Flight Dynamics, PT. Pasifik Satelit Nusantara. His research interests include GNSS Positioning, Satellite Navigation, Satellite Technology, and Orbital Mechanics. He can be contacted at email: djaka.ariya@psn.co.id.